THE JOURNAL OF PHYSICAL CHEMISTRY C

Article

pubs.acs.org/JPCC

CO Adsorption on Clean and Oxidized Pd(111)

N. M. Martin,[†] M. Van den Bossche,[‡] H. Grönbeck,[‡] C. Hakanoglu,[§] F. Zhang,[§] T. Li,[§] J. Gustafson,[†] J. F. Weaver,[§] and E. Lundgren*[,†]

[†]Division of Synchrotron Radiation Research, Lund University, 221 00 Lund, Sweden

[‡]Department of Applied Physics and Competence Centre for Catalysis, Chalmers University of Technology, 412 96 Göteborg, Sweden

[§]Department of Chemical Engineering, University of Florida, Gainesville, Florida 32611, United States

ABSTRACT: The adsorption of CO on clean and oxidized Pd(111) surfaces has been investigated using a combination of high-resolution core level spectroscopy (HRCLS), reflection absorption infrared spectroscopy (RAIRS), and density functional theory (DFT) calculations. The HRCLS and RAIRS measurements reveal that CO adsorbs on Pd(111), Pd_5O_4 and PdO(101) at 100 ± 10 K and that the CO coverage decreases with increasing oxidation state of Pd for the same CO exposures of 10 Langmuirs. Based on the DFT calculations, the CO layer on clean Pd(111) was found to include molecular adsorption in both hollow and bridge sites, whereas CO occupies a combination of bridge and atop sites on the Pd_5O_4 and PdO(101) surfaces.

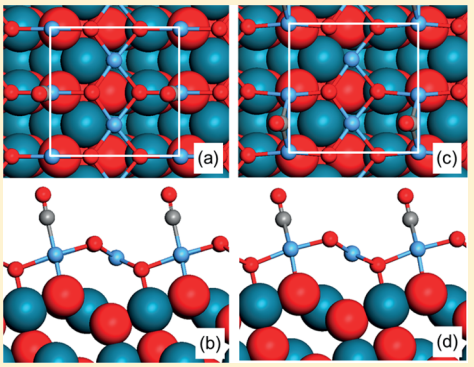

I. INTRODUCTION

Pd is an important catalyst for commercial oxidation processes such as the catalytic oxidation of methane in gas turbines and the oxidation of hydrocarbons and CO in automotive exhausts.[1] CO oxidation is one of the most widely studied reactions in heterogeneous catalysis, and the interaction of CO with different metal and metal oxide surfaces has been extensively investigated during the past 40 years as a part in improving the understanding of the oxidation reaction.[2−13] CO is known to adsorb molecularly via the carbon atom to surfaces of the late transition metals. The molecule binds to surfaces via a concerted mechanism where the highest occupied molecular orbital (HOMO) is coordinated to the surface (5σ donation) and simultaneously the lowest unoccupied molecular orbital (LUMO) is populated by charge transfer from the surface ($2\pi^*$ back-donation).[14,15] It should be noted that palladium is easily oxidized and that surface oxide or oxide phases have been observed during typical reaction conditions. Thus, it is also important to explore the interaction of CO with different oxide phases.

A variety of experimental techniques have been employed to study the CO/Pd(111) system including infrared reflection−absorption spectroscopy (IRAS),[16−18] low energy electron diffraction (LEED),[19] photoelectron diffraction,[20] high-resolution core level spectroscopy (HRCLS), electron energy loss spectroscopy (EELS),[21] and scanning tunneling microscopy (STM).[22]

The studies show that the surface structure of CO overlayers on Pd(111) are coverage-dependent where $(\sqrt{3} \times \sqrt{3})R30°$ and c(4 × 2)-2CO phases are formed at coverages of 0.33 monolayers (ML) and 0.5 ML, respectively, whereas a (2 × 2)-3CO structure can form at higher coverages (0.75 ML). The early results from vibrational spectroscopy suggested that CO adsorbs in 3-fold hollow sites in the $(\sqrt{3} \times \sqrt{3})R30°$ phase and in bridge sites in the c(4 × 2)-2CO phase.[2,16] The assignment of the structure in the c(4 × 2)-2CO phase has, however, been questioned in later studies. A photoelectron diffraction study by Gießel et al.[20] suggested that CO adsorbs in a mixture of face-centered cubic (fcc) and hexagonal close-packed (hcp) sites in the c(4 × 2) phase rather than the bridge sites, while an STM study by Rose et al.[22] reported the coexistence of c(4 × 2) domains in which CO assumes either only bridge sites or a combination of fcc and hcp hollow sites. For the higher coverage (2 × 2)-3CO structure, CO has been reported to occupy both the 3-fold hollow and atop sites.[2,17] The previous reports demonstrate that a full understanding of CO adsorption on Pd(111) is still missing and that it actually is a challenge to obtain a complete picture of the bonding geometry.

Oxidation of Pd(111) with molecular oxygen leads initially to the formation of a p(2 × 2) structure (0.25 ML coverage) and at higher coverages (0.67 ML) to a two-dimensional (2D) oxide ($(\sqrt{6} \times \sqrt{6})$) with a Pd_5O_4 stoichiometry.[23,24] Here, 1 ML equals the surface atom density of Pd(111). Bulk Pd oxidation has been found to proceed through PdO seeds that grow on the 2D oxide.[25,26] Furthermore, it has been shown that a well-ordered PdO(101) film can form under ultrahigh vacuum (UHV) conditions by oxidation of Pd(111) with

Received: November 5, 2013
Revised: December 17, 2013
Published: December 17, 2013

   dx.doi.org/10.1021/jp410895c | J. Phys. Chem. C 2014, 118, 1118−1128

atomic oxygen.[27,25] The detailed XPS signatures from such a PdO(101) film have recently been reported.[28]

Also the interaction of CO with oxidized Pd(111) has been investigated previously. In a recent HRCLS study performed at 290 K,[29] it was shown that exposure of the p(2 × 2)-O/Pd(111) structure to CO resulted in a compression of the oxygen overlayer to first a $(\sqrt{3} \times \sqrt{3})R30°$ phase and at higher CO doses, to a p(2 × 1) phase. In addition, it was shown in a recent combined LEED and DFT study that the exposure of the p(2 × 2)-O/Pd(111) structure at 200 K to CO resulted in a compression of the oxygen overlayer to a $(\sqrt{3} \times \sqrt{3})R30°$ phase.[30] The interaction of CO with PdO(101) has been studied both theoretically and experimentally. A recent theoretical study by Hirvi et al.[31] reports that CO adsorbs strongly on the PdO(101) surface and that CO oxidation may proceed via a Mars-van Krevelen mechanism. For PdO(100), which is predicted to be the stable PdO surface, CO was instead found to adsorb weakly and the CO oxidation was suggested to follow an Eley−Rideal (ER) path. These results are in agreement with other theoretical reports[32,33] as well as experiments. In a TPD study by Hinojosa et al.,[34] it was reported that CO adsorbs molecularly on the PdO(101) surface at 85 K and that more than half of the adsorbed CO reacts with oxygen atoms from the PdO surface, forming CO_2 that desorbs in a peak at around 355 K. This is indicative of a Mars-van Krevelen mechanism. In ref 34, a saturation coverage for CO of 0.35 ML was measured on PdO(101). This coverage is equal to the concentration of undercoordinated Pd atoms in the surface. These atoms (Pd_{3f}), are coordinated to only three oxygen atoms, whereas Pd in the bulk of PdO has four oxygen neighbors (Pd_{4f}). That the CO coverage and Pd_{3f} concentration coincide suggest that CO adsorbs preferentially on Pd_{3f} sites and that all available sites are occupied at saturation. This assumption is supported by a recent combined high pressure X-ray photoelectron spectroscopy (HPXPS) and density functional theory (DFT) study of the oxidation with molecular oxygen and oxide reduction with CO on Pd(100) and Pd nanoparticles.[33]

In the present study, we have investigated the interaction of CO with clean as well as oxidized Pd(111) surfaces (the surface oxide Pd_5O_4 and the PdO(101) surface) at liquid nitrogen temperature using a combination of HRCLS, RAIRS and DFT calculations. The HRCLS measurements show that CO adsorbs on all structures but has different coverages for the same CO exposures. In good agreement with previous studies, a c(4 × 2) structure was found to form upon CO adsorption on Pd(111) to a coverage of 0.5 ML. Upon exposing the Pd_5O_4 and PdO(101) surfaces to the same amount of CO, the binding energy of C 1s was found to be sensitive to the oxidation state of the surface, and a shift of 0.3 and 2 eV was measured for the Pd_5O_4 and PdO(101) surface, respectively. The present study shows that the adsorption sites occupied by CO on the different surfaces change from the hollow and bridge sites on clean Pd(111) to bridge and atop sites on the oxidized Pd surfaces. This phenomenon has previously been discussed in ref 35. Moreover, the CO coverage is found to decrease with increased oxidation state of Pd.

II. EXPERIMENTAL METHODS

A. HRCLS Measurements. The HRCLS measurements were performed at beamline I311 at the MAX IV Laboratory in Lund, Sweden.[36] The Pd(111) single crystal used in the experiments was mounted on a tungsten wire through which it could be heated to high temperatures by applying an electric current. The temperature of the sample was measured by a Chromel-Alumel thermocouple spot-welded on the back side of the crystal. The sample could be cooled to 100 K via liquid nitrogen cooling. The sample was cleaned by repeated cycles of sputtering with Ar^+ ions and annealing up to 1100 K and subsequent oxygen treatment with 1×10^{-7} mbar O_2 up to 970 K. The surface was checked by LEED and HRCLS.

The Pd_5O_4 structure was obtained by exposing the Pd(111) surface to molecular oxygen (5×10^{-6} mbar) at 575 K for 300 s.[37] For the preparation of the PdO film, the same methods were used as in our recent publication.[28] The Pd(111) surface was oxidized by atomic oxygen, produced by a thermal gas cracker (5×10^{-7} mbar), at a sample temperature of 500 K for 60 min. The CO adsorption measurements were performed at a sample temperature of 100 K. The CO gas used in the experiments was a commercially available research grade CO from Air Liquide with a purity of 99.94%. All surfaces were exposed to a CO dose of 10 L (1 L = 1 s at 10^{-6} mbar).

The HRCLS measurements were recorded using normal emission and photon energies of 380 eV for Pd 3d, 650 eV for O 1s and 435 eV for the C 1s states, respectively. For the analysis of the recorded HRCL spectra, a deconvolution procedure with a Doniach Šunjić line shape convoluted with a Gaussian was used. The binding energies were calibrated to the Fermi edge. All spectra are normalized to the background.

B. RAIRS Measurements. The RAIRS measurements were performed at the University of Florida in a UHV chamber with a typical base pressure of 3.33×10^{-10} mbar. Details of the UHV chamber will be provided in a coming publication. In brief, the UHV system is equipped with a Bruker Tensor 27 Fourier transform infrared spectrometer (FTIR), a shielded quadrupole mass spectrometer (Hiden), and a single-stage differentially pumped chamber[38] that houses a RF plasma source (Specs) that is used to generate atomic oxygen beams. The FTIR spectrometer is equipped with a mid-IR (globar) source and uses an external liquid N_2-cooled HgCdTe (MCT) detector.

Outside of the UHV chamber, the mid-IR (MIR) beam transmits within a sealed box that is continuously purged with H_2O and CO_2-free compressed air. The MIR beam is directed by a set of flat mirrors before impinging onto a parabolic mirror which focuses the MIR beam onto the sample. The focused MIR beam transmits into the UHV chamber through a differentially pumped KBr window and impinges on the sample surface at an angle of about 80° relative to the surface normal. The reflected MIR beam exits the chamber through a second KBr window and is directed onto the MCT detector using focusing mirrors, all of which are located in a separate box that is continuously purged with dry and CO_2-free air. Each spectrum was acquired using 256 scans at a resolution of 4 cm^{-1}, and required around 2 min to collect. Averaging more scans did not significantly improve the signal-to-noise ratio in the RAIRS data presented here.

In the RAIRS experiments, the Pd(111) surface was initially cleaned by Ar^+ sputtering at 823 K followed by annealing at 1100 K. Subsequent cleaning involved exposure of the Pd(111) surface (held at 856 K) to a plasma-generated oxygen beam, followed by temperature flashes to 1000 K to remove carbon contamination from the surface.

The Pd_5O_4 layer was prepared by exposing Pd(111) to an atomic oxygen beam for 180 s at 583 K. These preparation conditions place the Pd(111) oxidation kinetics in the so-called

dx.doi.org/10.1021/jp410895c | J. Phys. Chem. C 2014, 118, 1118−1128

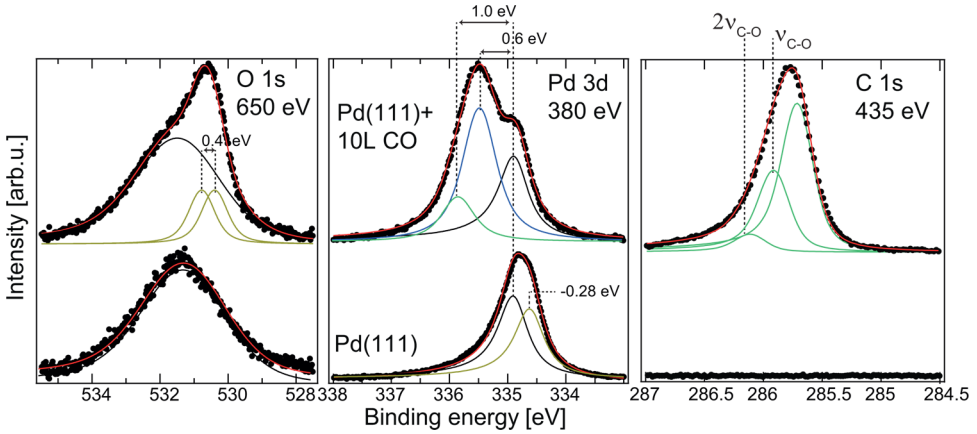

Figure 1. (Lower panel) HRCLS signature of clean Pd(111). In the Pd $3d_{5/2}$ signal, a contribution from a surface component (brown) is observed in addition to the bulk component (black). The O 1s signal is overlapping with the Pd $3p_{3/2}$ level. (Upper panel) O 1s, Pd $3d_{5/2}$ and C 1s HRCL spectra after dosing 10 L of CO on the Pd(111) surface at 100 ± 10 K. As CO adsorbs, the surface component in Pd $3d_{5/2}$ disappears, and two new components arise at higher binding energies (blue and green). In O 1s, two peaks are observed shifted by 0.4 eV. A single strong peak is observed in C 1s.

metastable regime wherein the oxygen uptake temporarily plateaus once a well-ordered Pd_5O_4 layer saturates.[25] The PdO(101) film was prepared by exposing clean Pd(111) at 433 K to atomic oxygen for 30 min, followed by annealing at 533 K. The surface prepared under this condition has an oxygen coverage of 3.7 ML.

We performed temperature programmed desorption (TPD) measurements to estimate initial oxygen and CO coverages on the surfaces under study. The TPD experiments were performed by positioning the Pd(111) sample at a distance of about 3 mm from the entrance aperture of the mass spectrometer and heating at a constant rate of 1 K/s. The mass spectrometer is covered with a conical Feulner cap that has an entrance aperture of 6 mm diameter. Oxygen coverages are estimated by scaling O_2 TPD spectra obtained after generating a Pd_5O_4 layer on Pd(111) and assuming that the atomic oxygen coverage is 0.7 ML.[25] The CO desorption yield measured in TPD is estimated by scaling CO TPD spectra obtained after saturating Pd(111) with CO at 300 K and assuming that the saturation coverage is 0.55 ML.[21,39−42] Lastly, the desorption yields of CO_2 are estimated from CO_2 TPD data obtained from TPD experiments of CO oxidation on Pd(111) performed under conditions in which adsorbed atomic oxygen is the limiting reactant. In this case, the desorption yields of CO_2 are equal to the initial atomic oxygen coverages. Based on the TPD data, we estimate saturation coverages of 0.53, 0.46 and 0.35 ML for CO adsorbed on the Pd(111), Pd_5O_4 and PdO(101) surfaces at 100 K, respectively.

RAIRS data were in all cases collected at about 100 K after exposing the surface to a background dose of 10 L of CO at the same temperature. A 10 L exposure was sufficient to saturate each of the surfaces under study with CO at about 100 K.

III. COMPUTATIONAL METHOD

The density functional theory (DFT) was applied with the gradient-corrected exchange-correlation functional according to Perdew, Burke, and Ernzerhof (PBE).[43] In particular, the plane-wave pseudopotential code VASP was used.[44−46] The kinetic energy cutoff for the basis set was set to 450 eV. Standard PAW potentials[47,48] were used to treat the interaction between the valence electrons and the core. Reciprocal space integration over the Brillouin zone was approximated with finite sampling using Monkhorst−Pack grids[49,50] corresponding to 12 × 12 × 12 in the unit cell of bulk Pd and 8 × 8 × 6 in the unit cell of bulk PdO. For the surface oxide on Pd(111), the surface cell consists of seven Pd_5O_4 units supported on three Pd(111) layers with 48 atoms in each layer. This cell was sampled by a 3 × 1 × 1 k-point mesh. Geometry optimizations were carried out without any constraints, and the structures were considered relaxed when the largest force in the system was smaller than 0.01 eV/Å. Successive slabs in the direction normal to the surface were separated by at least 12 Å. The core-level shifts (CLS) were evaluated in a complete screening picture, including both initial and final state effects.[51] This was done by using pseudopotentials generated with an electron hole in either the 3d shell (Pd) or the 1s shell (C and O). The CLS were calculated with respect to a bulk reference, represented by an atom in the center of the slab (the middle layer). To maintain charge neutrality, a homogeneous jellium background was included. In order to ensure proper bulk references, seven Pd layers were used for the Pd(111) surface, five Pd substrate layers for the surface oxide and seven trilayers for the PdO(101) surface.

The C−O stretching frequencies were calculated using the harmonic approximation with a central difference scheme with 0.01 Å displacements of the adsorbate atoms. The partial Hessian approach was found to be justified for all three surfaces. The calculated frequencies are well converged with respect to the slab thickness for five Pd layers for the Pd(111) surface, three Pd substrate layers for the surface oxide and four PdO trilayers for the PdO(101) surface. In order to improve the comparison between the experimental and calculated frequencies, a scaling factor of 1.0238 was applied to the PBE frequencies, which was chosen such that the scaled calculated harmonic C−O stretching frequency in the gas-phase equals the experimental value (2170 cm^{-1}).[52] Experimentally, the anharmonic vibrational frequency is 2143 cm^{-1}.[53]

IV. RESULTS

A. HRCLS of CO adsorption on Pd(111). The O 1s, Pd $3d_{5/2}$ and C 1s levels were recorded at normal emission, and the results for the clean Pd(111) sample are shown in Figure 1, lower panel. The peak in the O 1s region at 531.5 eV (black) originates from the Pd $3p_{3/2}$ level. The Pd $3d_{5/2}$ signal can be

dx.doi.org/10.1021/jp410895c | J. Phys. Chem. C 2014, 118, 1118−1128

deconvoluted with two components assigned to bulk (334.9 eV, black) and surface (334.6 eV, brown) atoms, respectively. In the upper panel of the figure, we present the O 1s, Pd $3d_{5/2}$, and C 1s levels after dosing 10 L of CO at 100 ± 10 K on a clean Pd(111) surface. The shifts of the different components in the Pd $3d_{5/2}$ are given with respect to the metal bulk Pd.

The C 1s signal shows that CO adsorbs on Pd(111) at about 100 K and has a peak at 285.6 eV. Two additional components, marked ν_{C-O} and $2\nu_{C-O}$, are coupled to the main peak and originate from excitation of C−O stretch vibrations in the photoemission process. The vibrational components have binding energies shifted by 0.2 and 0.4 eV and intensities of 0.55 and 0.12 relative to the main component, respectively.[21] Upon CO exposure, the surface component of Pd $3d_{5/2}$ is affected, and two new components appear, shifted by 0.6 (blue) and 1.0 eV (green) toward higher binding energy with respect to the bulk signal. The deconvolution of the O 1s from adsorbed CO is clearly difficult, but can be made using two components at about 530.9 and 531.3 eV (both brown). The present results for the Pd $3d_{5/2}$ and C 1s binding energies are in good agreement with the previous HRCLS study of CO adsorption on Pd(111)[21] reported for a 0.5 ML coverage corresponding to the c(4 × 2) structure. Based on this, it can be assumed that the CO coverage is close to 0.5 ML on Pd(111) under the present experimental conditions. We use this value as a reference to calculate the experimental coverages of CO on the surface oxide and the PdO(101) film (see below). In the HRCLS study by Surnev et al.,[21] the CO molecules in the c(4 × 2) structure were suggested to be adsorbed in 3-fold hollow positions. By contrast, the STM measurements by Rose et al.[22] for a coverage of 0.5 ML, suggest that there is a mixed phase consisting of CO bound in 3-fold hollow and bridge sites.

Because of the contradictory reports regarding the adsorption sites of CO in the c(4 × 2) structure, a set of DFT calculations for CO adsorption on Pd(111) was performed. Although different coverages were considered, we concentrate on results for 0.5 ML in a c(4 × 2) surface cell. The optimized geometries of four different structures are presented in Figure 2. The calculated average adsorption energy together with the core level shifts (CLS) for the O, Pd, and C atoms are reported in Table 1. The Pd 3d shifts are calculated with respect to a Pd atom in the middle of the slab (bulk reference), whereas the C 1s and O 1s are calculated with respect to a CO molecule adsorbed in an hcp site on the opposite side of the slab.

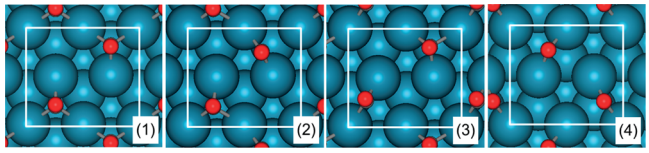

Figure 2. Left: Top view of the considered c(4 × 2) structures of CO on Pd(111). CO is in the different structures adsorbed in fcc-hcp (1), fcc-bridge (2), hcp-bridge (3), and bridge−bridge (4). The surface cell is indicated by white lines. Atomic color codes: Pd (blue), O (red), and C (gray).

The differences in stability of the considered c(4 × 2) structures are too small to allow for conclusions regarding the experimentally observed structure. Instead, the calculated CLSs give information on the most probable structure. Among the evaluated structures, the combined hollow-bridge geometries (configurations 2 and 3) agree best with the experimental data. The two structures, either hcp-bridge or fcc-bridge, have very similar core level binding energies and are not distinguishable by XPS alone.

Considering first the Pd 3d shifts, the two hollow-bridge structures have two different types of surface atoms: three Pd atoms are coordinated to one CO molecule, and one Pd atom is coordinated to two CO molecules. The atoms coordinated to one CO molecule have an average CLS of 0.56 eV, whereas the atom coordinated to two CO molecules has a CLS of 1.0 eV. The experimentally resolved CLSs are 0.6 and 1.0 eV, respectively. The intensity in the XPS signal corresponds naively to the number of atoms with a certain binding energy. The calculated ratio between the two types of Pd surface atoms is 1:3, which agrees with the 0.33 intensity ratio observed experimentally. For the O 1s binding energies, the hollow-bridge configuration has a shift of 0.4 eV, in good agreement with the experiments, although the experimental deconvolution is not unambiguously determined. The small difference in the predicted binding energies for C 1s (0.15 eV) is not possible to resolve experimentally, and only a single peak is observed.

The present interpretation differs from the one in ref 21, where it was suggested that the two CO molecules in the c(4 × 2) cell occupy only hcp and fcc sites. We note that such a structure does not give the experimentally observed 0.4 eV shift in O 1s and predict an 1:1 intensity ratio between the Pd 3d components.

B. HRCLS of CO adsorption on Pd_5O_4. The Pd_5O_4 surface oxide has previously been characterized experimentally with HRCLS, XRD, STM, LEED, and the structure has been determined by comparisons with DFT calculations.[23,37] The surface oxide has two types of Pd atoms, which are either 2- or 4-fold coordinated to O atoms and two types of O atoms which are either 3- or 4-fold coordinated to Pd atoms (see Figure 4). Our HRCLS results for the clean Pd_5O_4/Pd(111) surface are shown in the lower panel of Figure 3 as a reference. The Pd $3d_{5/2}$ spectrum was deconvoluted with three peaks, which are assigned to bulk Pd atoms (334.9 eV), Pd atoms coordinated to 2 O atoms (+0.6 eV with respect to the bulk component), and

Table 1. Calculated Adsorption Energies Together with O 1s, Pd 3d, and C 1s CLSs for the Considered c(4 × 2) Structures of CO on Pd(111)[a]

			O 1s		Pd 3d				C 1s	
configuration	adsorption sites	E_{ads}	I	II	I	II	III	IV	I	II
1	fcc-hcp	−1.82	+0.13	+0.14	+0.93	+0.90	+0.42	+0.43	+0.05	+0.06
2	hcp-bridge	−1.75	+0.53	+0.13	+1.00	+0.66	+0.53	+0.48	+0.22	+0.07
3	fcc-bridge	−1.76	+0.49	+0.14	+0.99	+0.65	+0.58	+0.46	+0.20	+0.06
4	bridge−bridge	−1.75	+0.43	+0.42	+0.69	+0.69	+0.60	+0.60	+0.22	+0.21

[a]The Pd 3d shifts are calculated with a bulk like Pd atom from the mid layer in the slab as a reference. The carbon and oxygen references are the atoms in a CO molecule adsorbed in an hcp site on the opposite side of the slab. All energies are reported in eV.

dx.doi.org/10.1021/jp410895c | J. Phys. Chem. C 2014, 118, 1118−1128

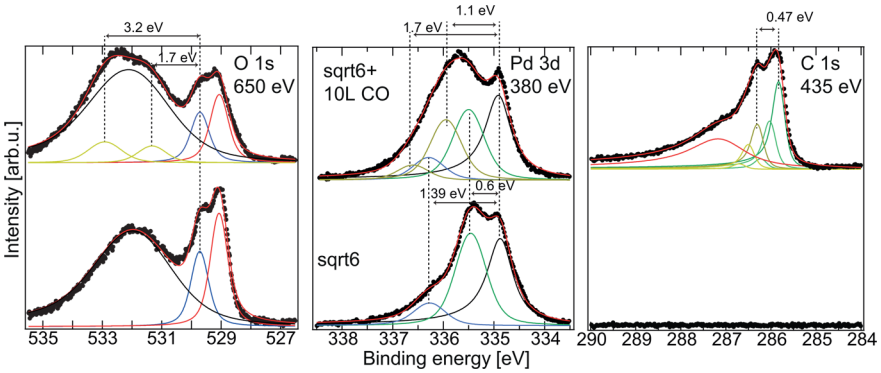

Figure 3. (Lower panel) HRCLS signatures of the Pd_5O_4 surface oxide grown on Pd(111). (Upper panel) HRCL spectra after dosing 10 L of CO on the surface oxide at 100 ± 10 K. As CO adsorbs, the component assigned to 2-fold coordinated Pd atoms in Pd $3d_{5/2}$ decreases and two new components appear at about 1.1 and 1.7 eV toward higher binding energy (brown). The O 1s and C 1s spectra also have CO induced components.

Pd atoms coordinated to 4 O atoms (+1.4 eV). The ratio of the intensities between the peaks are consistent with the ratio between the number of 4-fold and 2-fold atoms in the surface cell, namely, 7:28. In addition to the Pd $3p_{3/2}$ peak near 531.5 eV, the O 1s level presents an oxide feature that could be decomposed into two components with a difference in binding energy of 0.66 eV. The two peaks are assigned to O atoms that are 3- (red) or 4-fold (blue) coordinated to Pd atoms. The CLSs of the clean Pd_5O_4 structure were also investigated computationally. The 2-fold and 4-fold Pd atoms were calculated to be shifted by +0.60 and +0.96 eV with respect to the bulk reference, respectively. The shift between the two oxygen atoms was calculated to be 0.57 eV with the highest binding energy of the 4-fold coordinated atom. The results are in full agreement with the previously reported calculations.[37] The underestimation of the shift for the Pd atom coordinated to four oxygen atoms could, at least in part, originate from the used approximation to the exchange-correlation functional.[54]

CO adsorption was investigated after the Pd_5O_4 reference system was established. In the upper panel of Figure 3, the core level spectra are presented after 10 L of CO exposure at 100 K. The spectra clearly show that CO adsorbs under these conditions. In the O 1s spectrum, two new components at about 531.4 and 532.9 eV are observed. In the Pd $3d_{5/2}$ spectrum, the component assigned to the 2-fold coordinated Pd atoms decreases, and new components appear at 1.1 and 1.7 eV toward higher binding energies (with respect to the Pd atoms in the metallic bulk Pd). The component assigned to the 4-fold coordinated Pd atoms is unchanged, which implies that those atoms are not directly involved in the CO adsorption. A broad peak is observed in C 1s, which could be decomposed with three main components and additional vibrational components. The origin of the high binding energy component (red, at about 287 eV) is presently not fully understood, but it may originate from CO adsorbed on imperfect areas of the Pd_5O_4 surface as supported by the RAIRS data (see below). The other two components, separated by 0.47 eV can be assigned to CO adsorbed at different sites. Each component is coupled to two additional vibrational components just as in the case for CO molecules adsorbed on Pd(111). From the intensity of the C 1s, we estimate the CO coverage to be 0.29 ML with respect to Pd(111). Here it should be noted that a CO coverage estimation using a single photon energy for CO at different sites could lead to a relatively large error.[56]

A broad CO component at around 287 eV was previously observed during the CO-induced reduction of PdO grown on Pd(100)[33] and it was assigned to CO on a PdO(101) surface occupying both atop and bridge sites. This assignment will be further discussed below. Furthermore, IR studies of CO adsorption on the $\sqrt{5} \times \sqrt{5}$ surface oxide on Pd(100) (hereafter denoted "root5") suggested that CO on this system may adsorb in both atop and bridge sites.[57]

A set of DFT calculations was performed to elucidate the adsorption of CO on the Pd_5O_4 surface oxide. Five different adsorption sites were considered, namely atop a 2-fold Pd atom, atop a 4-fold Pd atom, bridge between 2-fold Pd atoms (two possibilities: bridge-A and bridge-B), and a hollow position formed by four 2-fold Pd atoms. CO only adsorbs in such 4-fold hollow positions if there is a subsurface Pd atom located directly underneath. This occurs in one out of seven Pd_5O_4 units. The different sites are indicated in Figure 4. The

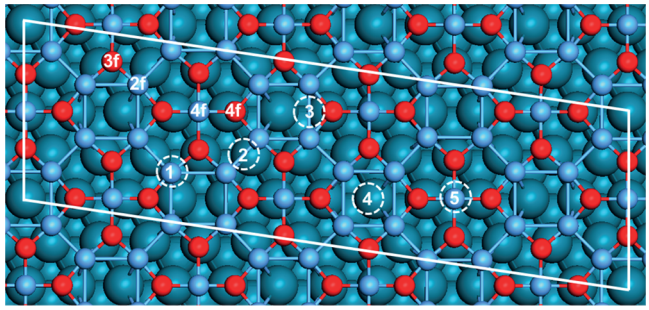

Figure 4. Top view of the relaxed Pd_5O_4 surface oxide. The surface cell and the investigated CO adsorption sites are indicated by a white parallelogram and white circles, respectively. Atomic color codes: Pd in surface oxide (light blue), Pd in unreconstructed surface (blue), O (red).

adsorption energies are presented in Table 2. The preferred adsorption site is bridge-A (site 2), followed by atop 2-fold (site 1), bridge-B (site 3) and the hollow site (site 4). The adsorption energy of CO atop the 4-fold Pd atom is close to zero, and we will in the following disregard this site. The computational results are in line with previous DFT studies of CO adsorption on the "root5" surface oxide,[33,58] where it has been shown that CO preferably adsorbs in bridge sites between 2-fold coordinated Pd atoms followed by atop adsorption on the same type of atoms. We note that the adsorption energies on Pd_5O_4 are lower than on the metal surface.

The calculated CLSs for O, Pd, and C with CO adsorbed in the different sites are collected in Table 2. The shift in the Pd

dx.doi.org/10.1021/jp410895c | J. Phys. Chem. C 2014, 118, 1118−1128

Table 2. Calculated Adsorption Energies and O 1s, Pd 3d, and C 1s CLSs for the Different CO Adsorption Sites on the Pd_5O_4 Surface Oxide[a]

adsorption site	E_{ads}	O 1s (CO)	Pd 3d (2f)	C 1s (CO)
atop-2f	−0.59	+3.16	+1.52	0.88
bridge-A	−1.00	+2.07	+1.27	0.43
bridge-B	−0.55	+1.82	+1.08	0.16
hollow	−0.20	+1.22	+1.07	0.21

[a]The Pd 3d shifts are calculated with respect to a bulk reference in the center of the slab. The C 1s shift is evaluated with respect to carbon in a CO molecule adsorbed on a hcp site on the opposite side of the slab. The O 1s shift is evaluated with respect to a 4-fold oxygen atom in the surface oxide.

3d spectrum (with respect to Pd in the metallic bulk) is sensitive to the adsorption configuration. The largest shift is predicted for CO in the atop-2f position followed by CO in the bridge-A position. The bridge-B and hollow positions generate similar shifts. Experimentally, there is a prominent peak at +1.1 eV and a smaller peak at +1.7 eV. For the large Pd 3d shift, CO adsorbed on atop-2f sites is the best candidate. Given the low adsorption energy at the hollow site, we tentatively assign the smaller Pd 3d shift of +1.1 eV to CO bonded in bridge configurations. As the bridge-A site has the highest adsorption energy, it can be argued that the smaller Pd 3d shift mainly arises from bridge-A and that a smaller contribution to this peak could be due to bridge-B. The small calculated shift between bridge-A and bridge-B can not be resolved experimentally. Turning to the O 1s spectrum, the experiments show two new components at +1.7 and +3.2 eV with respect to the 4-fold O reference. Those shifts match the calculated +1.9 eV and +3.16 eV shifts for bridge (average A and B) and atop, respectively. The experimental C 1s spectrum shows two peaks which are separated by about 0.5 eV. We calculate a similar difference between the average bridge shift and atop (0.45 eV).

On the Pd_5O_4 surface oxide, we conclude that CO adsorbs on both atop and bridge configurations, with a preference for the bridge sites. The C 1s spectrum suggests a bridge-A configuration, whereas the Pd 3d spectrum suggests a bridge-B configuration. The RAIRS data presented below show features consistent with a high coverage of bridge-CO species and a smaller coverage of atop-CO adsorbates.

C. HRCLS of CO Adsorption on PdO(101)/Pd(111). The PdO(101) film has previously been investigated both experimentally[25,27] and theoretically.[33,59,60] The film consists of alternating rows of Pd and O atoms which at the surface are either 3-fold or 4-fold coordinated. In a previous report, we presented a detailed combined HRCLS and DFT study of PdO(101) grown on Pd(111).[28] The O 1s, Pd $3d_{5/2}$ and C 1s spectra have been recorded at normal emission, and the results for the clean PdO(101) film on Pd(111) are shown in the lower panel of Figure 5. Two main peaks are present in the Pd $3d_{5/2}$ spectrum and are assigned to 3-fold coordinated surface atoms (Pd_{3f}, red) and 4-fold coordinated Pd atoms (Pd_{4f}, blue). Note that the spectrum is recorded at a low photon energy, which gives minor contribution from Pd in the bulk of the film. The oxide peak in the O 1s level is deconvoluted into two components assigned to the 3-fold (O_{3f}, red) or 4-fold (O_{4f}, blue) coordinated O atoms. As hydrogen from the chamber may easily adsorb and react with the PdO film after preparation, small $OH_{3f}/Pd_{3f}H$ components are present in the Pd $3d_{5/2}$ and O 1s/Pd $3p_{3/2}$ spectra (light blue). The peaks have previously been assigned to H bonded to the undercoordinated surface atoms.[28]

CO adsorption was investigated on the PdO(101) film at the same experimental conditions as for the Pd(111) and Pd_5O_4 surfaces and the resulting O 1s, Pd $3d_{5/2}$ and C 1s spectra are reported in the upper panel of Figure 5. The shifts are given with respect to the bulk metal Pd (Pd $3d_{5/2}$), or the 4-fold coordinated O atoms (O 1s). The measurements reveal that CO adsorbs on the PdO(101) surface. In the O 1s spectrum, a new component arises at about 534 eV. In Pd $3d_{5/2}$, the intensity of the Pd_{3f} component decreases (red) and two new components at 1.87 and 2.47 eV higher binding energy are observed (brown). The C 1s level shows a broad peak at 288.2 eV. The spectrum could be decomposed by two components shifted by 0.7 eV. Furthermore, a broad feature is observed at about 287 eV, similar to the CO on Pd_5O_4. This peak may arise from CO adsorbed on imperfect areas of the PdO(101) film or interaction between the CO and hydrogen adsorbed on the surface.

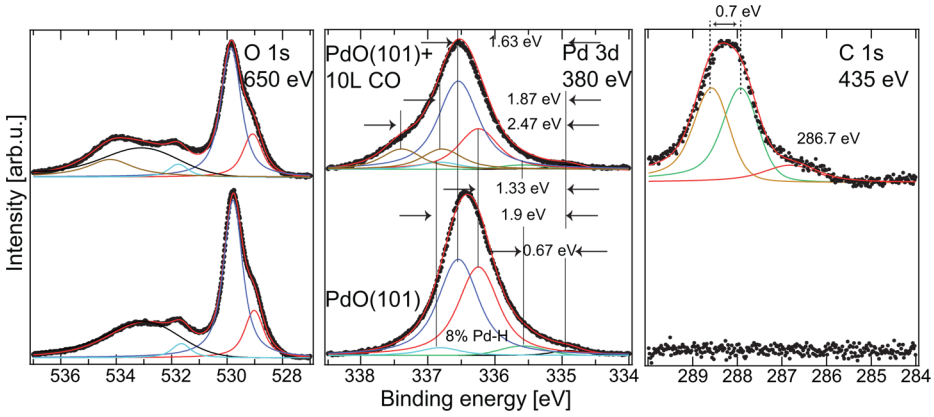

Figure 5. (Lower panel) HRCLS signature of the PdO(101) film grown on Pd(111). In the Pd $3d_{5/2}$ spectra, a contribution from a surface oxide (green), Pd−H (light blue) and Pd bulk component (black) may be observed. The shifts are given with respect to the bulk Pd (Pd $3d_{5/2}$). (Upper panel) O 1s, Pd $3d_{5/2}$ and C 1s HRCL spectra after dosing 10 L of CO on the PdO(101) surface at 100 ± 10 K. As CO adsorbs on PdO(101), the component from the undercoordinated Pd atoms (red) in Pd $3d_{5/2}$ level decreases, and two new components appear at higher binding energy (brown). A broad peak at about 288 eV is observed in C 1s and one new component around 534 eV is resolved in O 1s.

dx.doi.org/10.1021/jp410895c | J. Phys. Chem. C 2014, 118, 1118−1128

The measurements show that only the Pd_{3f} atoms at the surface of the oxide are affected by CO adsorption. As the best fit was obtained using two CO induced components in Pd $3d_{5/2}$, it suggests that CO adsorbs in two different configurations that involve Pd atoms on PdO(101). From the intensity of the C 1s level, the CO coverage can be estimated to be 0.17 ML in terms of Pd(111). However, again the CO coverage from this estimate may be affected by diffraction effects.[56]

DFT calculations of CO adsorption on PdO(101) were performed for different sites and coverages using a model with seven PdO trilayers. In particular, CO adsorbed in atop and/or bridge sites at coverages of 0.12, 0.17, 0.23, and 0.35 ML were considered. The calculated adsorption energies are reported in Table 3, and the relaxed structure for CO adsorbed atop and bridge at 0.17 ML coverage is shown in Figure 6. At coverages lower than 0.23 ML, the adsorption energy is found to vary moderately and the difference between atop and bridge is small. For a coverage of 0.23 ML, a mixed atop-bridge configuration is slightly preferred with respect to only atop or only bridge. The adsorption energy is calculated to be slightly smaller at full coverage with a preference for the atop site.

Table 3. Calculated Adsorption Energies of Different Configurations of CO on PdO(101) at Varying Coverage[a]

configuration	adsorption site(s)	coverage	E_{ads} (eV)
1	atop	0.17	−1.47
2	bridge	0.17	−1.46
3	atop	0.12	−1.49
4	bridge	0.12	−1.44
5	atop−atop	0.23	−1.44
6	bridge−bridge	0.23	−1.45
7	atop-bridge	0.23	−1.50
8	atop	0.35	−1.34
9	bridge	0.35	−1.21

[a]1 (one) ML equals the surface atom density of Pd(111).

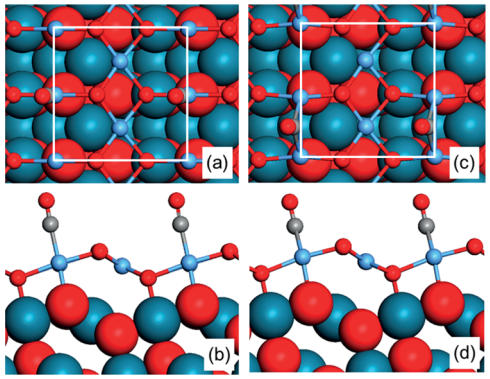

Figure 6. Top and side views of CO adsorbed atop (left) and bridge (right) on PdO(101) at 0.17 ML coverage. The surface cell is indicated by white lines. Atomic color codes: Pd (blue), O (red), C (gray).

The O 1s, Pd 3d, and C 1s core-level binding energy shifts were calculated for atoms in the topmost PdO(101) trilayer for all considered configurations. The results are collected in Table 4. Here, a zero shift for Pd, O, and C corresponds to Pd in bulk PdO, O in bulk PdO, and C in a CO molecule adsorbed on an atop site, respectively. We find that the calculated CLSs are very similar for coverages lower than 0.35 ML (full coverage = 1 CO adsorbate per 3-fold Pd surface atom). CO adsorbed in atop configuration yields a positive shift of +1.0 eV for the involved Pd atom, whereas CO adsorbed in a bridge configuration yields small negative shifts close to the position of Pd_{3f} except at full coverage, where the shift turns positive. In fact, this observation may explain why we do not observe a full attenuation of the Pd_{3f} component since CO in a bridge position yields a similar shift at coverages below full coverage. The CLSs for the surface O atoms do not change considerably upon CO adsorption. However, the oxygen in CO is shifted either 3 eV (atop) or 1.2 eV (bridge) with respect to O in the bulk PdO. The C 1s binding energy of CO adsorbed in bridge is typically 1 eV lower than for the case of CO adsorbed atop.

The experimental spectrum shows Pd $3d_{5/2}$ shifts around +0.8 eV and +0.2 eV, respectively. This agrees well with the calculated CLSs of Pd_{3f} with adsorbed CO on both atop and bridge configurations. We therefore assign the CO-induced components in Pd $3d_{5/2}$ spectrum to the Pd_{3f} + CO in bridge configuration (+0.2 eV shifted component with respect to Pd in PdO bulk) and Pd_{3f} + CO in atop configuration (+0.8 eV with respect to Pd in PdO bulk). The assignment of the O 1s components is more problematic as the experimental shift of the CO-induced component is larger than any of the shifts calculated within PBE.[54] As the largest shift toward higher binding energy is calculated for CO in the atop configuration, we assign the component at about 534 eV in O 1s to the O atoms from the CO adsorbed in an atop site on PdO(101). The lower binding energy components are not resolved experimentally, as they will overlap with the Pd 3p feature. The presence of both atop and bridge adsorbed CO is also consistent with the experimental C 1s spectrum, which shows two peaks shifted by about 0.7 eV.

D. RAIRS of CO adsorption on clean and oxidized Pd(111). RAIRS experiments were performed to provide additional support for the site assignments. The results are presented in Figure 7. For clean Pd(111), IR spectra were collected after exposing the surface to different amounts of CO at about 100 K. The changes that we observe in the IR spectra with increasing CO coverage agree well with prior IR studies[61,62] which show that CO initially adsorbs on hollow sites of Pd(111) and then begins to populate bridge sites, at least partially, as the coverage increases. The bottom of Figure 7 shows the IR spectrum obtained from a saturated CO layer prepared on Pd(111) at about 100 K. A strong peak is observed at 1959 cm^{-1} and smaller features are also apparent at 1864, 1900, 2091, and 2112 cm^{-1}. Based on TPD measurements, we estimate a saturation coverage of 0.53 ML for CO adsorbed on Pd(111) at 100 K under the conditions studied. Our estimated saturation coverage and the corresponding IR spectrum agree well with previously reported data[40,41] for CO adsorbed to saturation on Pd(111) at 100 K. The dominant IR peak at 1959 cm^{-1} has been previously attributed to CO adsorbed on bridging sites within the c(4 × 2) phase at coverages near 0.5 ML.[2,39,62] Notably, prior studies report that adsorbed CO can reach a coverage of 0.75 ML on Pd(111) at temperatures near 100 K by forming a (2 × 2)-3CO phase.[39,62] CO molecules bind on both atop and hollow sites in the (2 × 2)-3CO phase, resulting in an IR spectrum that is dominated by sharp peaks at 2111 cm^{-1} (atop) and 1896 cm^{-1} (hollow). We observe an IR spectrum that is characteristic of the (2 × 2)-3CO phase only after heating the Pd(111) surface to 150 K in a CO background

dx.doi.org/10.1021/jp410895c | J. Phys. Chem. C 2014, 118, 1118−1128

Table 4. Calculated O 1s, Pd 3d, and C 1s Core-Level Binding Energy Shifts for the Considered Structures of CO on the PdO(101) Surface[a]

		O 1s								Pd $3d_{5/2}$						C 1s	
		O(CO)		3-fold			4-fold			3-fold			4-fold			C(CO)	
n	adsorption site(s)	I	II	I	II	III	I	II	III	I	II	III	I	II	III	I	II
0	clean	-	-	−0.93	-	-	−0.33	-	-	−0.59	-	-	+0.12	-	-		
1	atop	+2.93	-	−0.90	−0.84	-	−0.25	−0.22	-	+1.04	−0.68	-	+0.13	+0.13	-	0	-
2	bridge	+1.11	-	−1.09	−1.09	-	−0.41	−0.41	-	−0.22	−0.20	-	+0.14	−0.01	-	−1.06	-
3	atop	+3.02	-	−0.9	−0.86	−0.86	−0.29	−0.29	−0.23	+1.06	−0.65	−0.64	+0.15	+0.11	+0.11	0	-
4	bridge	+1.20	-	−1.10	−1.10	−0.92	−0.40	−0.40	−0.35	−0.18	−0.18	−0.66	+0.17	+0.05	+0.05	−1.03	-
5	atop−atop	+3.07	-	−0.84	−0.84	−0.79	−0.22	−0.18	−0.18	+1.01	+1.01	−0.71	+0.17	+0.17	+0.07	0	-
6	bridge−bridge	+1.35	-	−1.16	−1.10	−1.10	−0.43	−0.41	−0.41	+0.11	+0.04	+0.04	+0.18	+0.18	−0.09	−0.96	-
7	atop−bridge	+2.97	+1.28	−1.04	−1.04	−0.88	−0.34	−0.34	−0.23	−0.17	−0.17	+1.04	+0.19	+0.04	+0.04	0	−0.98
8	atop	+3.04	-	−0.80	-	-	−0.13	-	-	+0.97	-	-	+0.13	-	-	0	-
9	bridge	+1.42	-	−0.92	-	-	−0.29	-	-	+0.47	-	-	+0.15	-	-	−0.86	-

[a]The Pd 3d and O 1s shifts are calculated with a bulk Pd atom from the middle trilayer as a reference. The carbon reference is a carbon atom in a CO molecule adsorbed in an atop site on the backside of the slab.

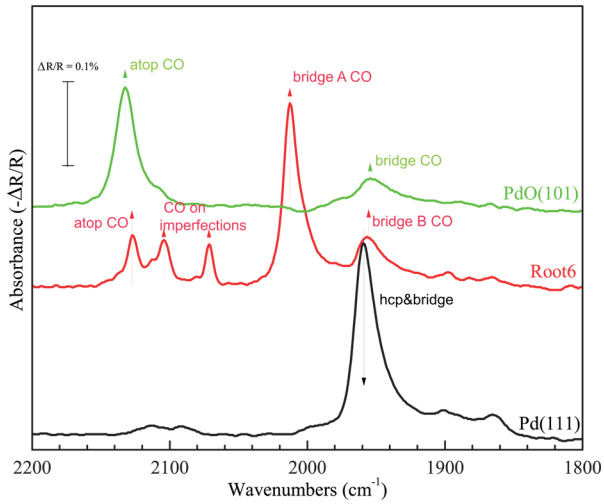

Figure 7. IR spectra collected at 100 K with 1.33×10^{-8} mbar CO background on Pd(111)-black, Pd_5O_4-red, and PdO(101)-green.

followed by cooling to 100 K. The behavior that we observe is consistent with results reported by Kuhn et al.[62] In ref 62 it was observed that a small peak at 2096 cm^{-1}, consistent with atop-CO, persists until the (2 × 2)-3CO phase saturates. We thus conclude that the saturated CO layer obtained on Pd(111) at 100 K predominantly consists of the c(4 × 2) phase, with only small amounts of higher density phases present. The CO molecules present in the c(4 × 2) phase give rise to the strong peak at 1959 cm^{-1} as well as the weaker peak at 1864 cm^{-1} (see below), while the weak features at 1900, 2091, and 2112 cm^{-1} originate from CO in high density phases. As discussed below, this finding agrees well with the HRCLS data which suggests that CO adsorbs on both 3-fold hollow and bridge sites of Pd(111) when exposed to 10 L CO at about 100 K.

DFT calculations were performed of the C−O stretch vibrations, and the results for the investigated c(4 × 2) configurations on Pd(111) are reported in Table 5. The calculations show that the hollow and bridge CO stretch vibrations are coupled, leading to symmetric and antisymmetric stretch modes. The intensities of the symmetric modes should be significantly larger than those of the antisymmetric modes owing to a considerably larger dynamical dipole moment. The

Table 5. Calculated C−O Stretch Frequencies for Different CO Overlayer Structures on the Pd(111) Surface at 0.5 ML Coverage

		stretch frequency (cm^{-1})	
	adsorption site	symmetric	antisymmetric
1	c(4 × 2)hcp-bridge	1957	1862
2	c(4 × 2)fcc-hcp	1917	1852
3	c(4 × 2)bridge−bridge	1964	1904

results for the c(4 × 2)-bridge+hollow structure has frequencies that are close to the measured values 1957 versus 1959 cm^{-1} and 1862 versus 1864 cm^{-1}, thus supporting the HRCLS assignment. The fact that this structure is compatible with the measured IR frequency is due to the aforementioned vibrational coupling and the strong coverage dependence of the stretch frequencies. The coverage dependence was investigated in a p(2 × 2) cell for the atop, bridge, and hollow sites and are reported in Table 6.

Table 6. Symmetric C−O Stretch Frequencies for CO on the Different Adsorption Sites on the Pd(111) Surface, Calculated at Different Coverages in a p(2 × 2) Unit Cell

	Coverage		
adsorption sites	0.25 ML	0.5 ML	0.75 ML
p(2 × 2) hcp	1838	1932	1992
p(2 × 2) fcc	1847	1930	1991
p(2 × 2) bridge	1914	1980	2024
p(2 × 2) atop	2102	2126	2143

For the Pd_5O_4 structure (Figure 7, mid panel) the peak at about 1959 cm^{-1} appears to reduce, broaden and slightly shift to 1957 cm^{-1} and a strong new peak is observed at 2012 cm^{-1}. Weaker peaks are also observed at higher frequencies: 2071, 2104, and 2127 cm^{-1}. A CO coverage of 0.46 ML is estimated from TPRS data after saturating the Pd_5O_4 surface with CO at about 100 K. The calculated frequencies of the C−O stretch vibrations for different structures of CO adsorbed on the Pd_5O_4 structure at both low (0.02 ML) and high (0.29 ML) coverages are collected in Table 7. We find that atop CO has the highest vibrational frequency, followed by bridge and hollow bound

dx.doi.org/10.1021/jp410895c | J. Phys. Chem. C 2014, 118, 1118−1128

Table 7. Calculated C−O Stretch Frequencies for Different Adsorption Configurations of CO on the Pd_5O_4 Surface at Low (1 CO per unit cell, 1/48 ML coverage) and High Coverages (0.29 ML)

	frequency (cm^{-1})	
adsorption site	0.02 ML	0.29 ML
atop	2109	-
bridge-A	1964	1997
bridge-B	1944	-
bridge-C	1846	-
hollow	1820	-

CO. The dominant peak observed at 2012 cm^{-1} is consistent with CO adsorbed on bridge-A sites at high coverage, whereas the peak at 1957 cm^{-1} is close to the calculated value for the bridge-B species at lower coverage. The minor peak at 2127 cm^{-1} likely arises from CO on 2-fold atop sites of the Pd_5O_4 structure, while the remaining small peaks at 2071 and 2104 cm^{-1} are difficult to assign. Similar peaks have been observed for atop CO on Pd(111) (2111 cm^{-1})[17,18] and after creating O-vacancies on PdO(101) (2070, 2111 cm^{-1}). The presence of these peaks in the IR spectra obtained from CO/Pd_5O_4 may indicate that the Pd_5O_4 layer is imperfect. Nevertheless, we see that the predominant atop and bridge bound CO adsorbates that best match the HRCLS data also explain the main features observed in the IR spectra.

For the CO-saturated PdO(101) surface (Figure 7, top panel), the RAIRS data presents two bands at 1955 cm^{-1} and 2132 cm^{-1}, which are consistent with CO adsorbed on bridge and atop sites, respectively. The saturation coverage estimated from TPD data is 0.35 ± 0.03 ML, in good agreement with TPD results reported previously.[34] The calculated frequencies (see Table 8) confirm that the IR absorption peaks at 2132 cm^{-1} and 1955 cm^{-1} correspond to atop and bridge bound CO, respectively, in agreement with the HRCLS experiments. The large width of the IR peak for bridge-bound CO on PdO(101) suggests that CO molecules adopt multiple orientations on the PdO(101) bridge sites. The integrated area ratio of the IR peaks for atop versus bridging CO species on PdO(101) is found to be 1.65 at the CO saturation coverage. However, it should be noted that IR peak intensities can depend sensitively on the local environment.[2,63]

Table 8. Calculated C−O Stretch Frequencies for CO Adsorbed on Atop and Bridge Sites at Four Different Coverages the PdO(101) Surface[a]

	frequency (cm^{-1})			
adsorption site	0.12 ML	0.17 ML	0.23 ML	0.35 ML
atop	2145	2146	2146	2162
bridge	1964	1978	2006	-

[a]A coverage of 1 ML corresponds to 1 CO molecule per one Pd surface atom of Pd(111).

From TPD data we estimate CO saturation coverages at about 100 K of 0.46 ML for Pd_5O_4 and 0.35 ML for PdO(101). These values are higher than the CO coverages calculated from the XPS data (0.29 ML for Pd_5O_4 and 0.17 ML for PdO(101)). As mentioned in our previous report,[28] the films may have imperfections or even different oxide orientations,[64] which may cause uncertainties with respect to the coverage estimation. As suggested in the interpretation of the IR data of CO on Pd_5O_4, two small peaks are observed that likely originate from CO on/near O-vacancies of the oxide or on-top of metallic Pd sites, which suggests that imperfections are present within the layer such as PdO(101) domains or metallic Pd sites.

V. DISCUSSION

In the present study, we have investigated CO adsorption on the Pd(111), Pd_5O_4, and PdO(101) surfaces. It is clear from the present and previous studies that CO adsorption is both complicated and rich concerning the adsorption sites and the exact geometries of the adsorption structures. Our results suggest that CO adsorbs in a mixture of hcp and bridge sites on Pd(111) at a coverage of 0.5 ML obtained at about 100 K, while, on Pd_5O_4 and PdO(101), CO adsorbs in a mixture of atop and bridge sites that are formed by the Pd_{2f} or Pd_{3f} sites, respectively. It is essential to emphasize the importance of the oxygen undercoordinated Pd atoms for the adsorption properties of Pd oxides, which is similar to the adsorption properties of the RuO_2(110) surface.[65,66] For comparison, oxidation of Rh results in a RhO_2 surface oxide with a fully closed top oxygen layer, on which no CO can be adsorbed even at 100 K.[67] The RAIRS data in Figure 7 are interesting to compare. First, it should be noted that interactions (dipole coupling) among adsorbed CO molecules cause the peak positions to change with the CO coverage. Coverage-dependent IR spectra for CO on Pd_5O_4 and PdO(101) will be published in a separate report. Although CO binds in similar adsorption sites on Pd_5O_4 and PdO(101) (atop and bridge), the spectra obtained from these oxide surfaces show significant differences in peak intensities and positions. For example, the dominant peaks assigned to bridge-bound CO appear at considerably different frequencies for the PdO(101) and Pd_5O_4 (bridge-A sites) surfaces (1955 vs 2012 cm^{-1}). In fact, since the peak at 2012 cm^{-1} is also distinct from features seen in the IR spectra obtained from Pd(111), this feature may provide a characteristic IR signature for identifying and distinguishing the Pd_5O_4 phase from Pd(111) and PdO(101) domains that could coexist during CO oxidation. Based on the current RAIRS measurements, it is tempting to assign 2142 and 2087 cm^{-1} peaks observed during CO oxidation on Pd(100) under O_2-excess conditions in a batch reactor to CO adsorbed on an oxidized Pd surface,[10] although low coverage atop sites could also be responsible for these peaks. Similar observations were reported for the Pd(111) and the Pd(110) surfaces in the same study. In that case it should be noted that the reaction rate was limited by CO diffusion to the surface, which also would facilitate the oxidation of the Pd surfaces.[68]

The finding of CO binding on cus-Pd sites agrees with a prior DFT study,[31] which predicts facile CO oxidation on PdO(101). The preferred and relatively strong binding of CO on the cus-Pd sites is also quite similar to the adsorption of CO on s-RuO_2(110). Thus, the CO oxidation behavior/mechanisms on PdO(101) and RuO_2(110) may exhibit common features. Further work is needed to explore these speculations. Furthermore, the calculations in ref 58 suggested that the surface oxide, the $(\sqrt{5} \times \sqrt{5})$, is active for the CO oxidation reaction on Pd(100) at technologically relevant conditions. Similar investigations have not yet been done for the $(\sqrt{6} \times \sqrt{6})$, and no experimental investigations at realistic conditions exist. Therefore it is difficult to compare the $(\sqrt{5} \times \sqrt{5})$ findings in ref 58 with the present UHV studies of CO adsorption on the $(\sqrt{6} \times \sqrt{6})$.

dx.doi.org/10.1021/jp410895c | J. Phys. Chem. C 2014, 118, 1118−1128

Finally it is interesting to note that a large shift of about 2.5 eV is observed in C 1s between CO/Pd(111) and CO/PdO(101), while the C 1s binding energy does not differ significantly between the Pd(111) and the Pd_5O_4 surfaces. The reason for the difference can be traced to differences in the CO-surface bond. This will be described in detail in a forthcoming publication.

VI. SUMMARY

The adsorption of CO at about 100 K on Pd(111), Pd_5O_4 and PdO(101) was studied by a combination of HRCLS, RAIRS and DFT. The main findings are as follows: (a) The c(4 × 2)-CO structure prepared on Pd(111) at about 100 K consists of CO adsorbed on both 3-fold hollow and bridge sites. (b) On the Pd_5O_4 surface, CO adsorbs on bridge and atop sites formed by Pd atoms coordinated to two oxygen atoms (Pd_{2f}). The bridge sites are preferably populated. (c) On PdO(101), CO adsorbs at close to equal preference on bridge and atop sites of Pd atoms coordinated to three oxygen atoms (Pd_{3f}).

VII. ACKNOWLEDGMENTS

The Max IV staff is gratefully acknowledged. This work was financially supported by the foundation for strategic research (SSF), the Swedish Research Council, the Crafoord Foundation, the Knut and Alice Wallenberg Foundation, the Anna and Edwin Berger Foundation and NordForsk. The Competence Centre for Catalysis (KCK) is hosted by Chalmers University of Technology and financially supported by the Swedish Energy Agency and the member companies: AB Volvo, ECAPS AB, Haldor Topsøe A/S, Scania CV AB and Volvo Car Corporation AB. The calculations were performed at C3SE (Göteborg and PDC (Stockholm) via a SNIC grant. J.F.W. gratefully acknowledges financial support provided by the U.S. Department of Energy, Office of Basic Energy Sciences, Catalysis Science Division, through Grant DE-FG02-03ER15478.

AUTHOR INFORMATION

Notes

The authors declare no competing financial interest.

REFERENCES

(1) Kaspar, J.; Fornasiero, P.; Hickey, N. Automotive catalytic converters: Current status and some perspectives. *Catal. Today* **2003**, *77*, 419−449.
(2) Hoffmann, F. M. Infrared Reflection-Absorption Spectroscopy of Adsorbed Molecules. *Surf. Sci. Rep* **1983**, *3*, 107−192.
(3) Somorjai, G. A. *Introduction to Surface Chemistry and Catalysis*; Wiley: New York, 1994.
(4) Ertl, G.; Knözinger, H.; Weitkamp, J. *Handbook of Heterogeneous Catalysis*; Wiley: New York, 1997.
(5) Nieuwenhuys, B. E. The Surface Science Approach toward Understanding Automotive Exhaust Conversion Catalysis at the Atomic Level. *Adv. Catal.* **1999**, *44*, 259−328.
(6) Zaera, F. Probing Catalytic Reactions at Surfaces. *Prog. Surf. Sci.* **2001**, *69*, 1−98.
(7) Hendriksen, B. L. M.; Bobaru, S. C.; Frenke, J. W. M. Oscillatory CO Oxidation on Pd(1 0 0) Studied with in Situ Scanning Tunneling Microscopy. *Surf. Sci.* **2004**, *552*, 229−242.
(8) Gustafson, J.; Westerström, R.; Mikkelsen, A.; Torrelles, X.; Balmes, O.; Bovet, N.; Andersen, J. N.; Baddeley, C. J.; Lundgren, E. Sensitivity of Catalysis to Surface Structure: The Example of CO Oxidation on Rh Under Realistic Conditions. *Phys. Rev. B* **2008**, *78*, 045423−1:6.
(9) Gustafson, J.; et al. Structure and Catalytic Reactivity of Rh Oxides. *Catal. Today* **2009**, *145*, 227−235.
(10) Gao, F.; Wang, Y.; Cai, Y.; Goodman, D. W. CO Oxidation on Pt-Group Metals From Ultrahigh Vacuum to Near Atmospheric Pressures. 2. Palladium and Platinum. *J. Phys. Chem. C* **2009**, *113*, 174−181.
(11) Gustafson, J.; Westerström, R.; Balmes, O.; Resta, A.; van Rijn, R.; Torrelles, X.; Herbschleb, C. T.; Frenken, J. W. M.; Lundgren, E. Catalytic Activity of the Rh Surface Oxide: CO Oxidation over Rh(111) under Realistic Conditions. *J. Phys. Chem. C* **2010**, *114*, 4580−4583.
(12) Van Rijn, R.; Balmes, O.; Resta, A.; Wermeille, D.; Westerström, R.; Gustafson, J.; Felici, R.; Lundgren, E.; Frenken, J. W. M. Surface Structure and Reactivity of Pd(100) During CO Oxidation Near Ambient Pressures. *Phys. Chem. Chem. Phys.* **2011**, *13*, 13167−13171.
(13) Blomberg, S.; et al. In Situ X-ray Photoelectron Spectroscopy of Model Catalysts: At the Edge of the Gap. *Phys. Rev. Lett.* **2013**, *110*, 117601−117605.
(14) Blyholder, G. Molecular Orbital View of Chemisorbed Carbon Monoxide. *J. Phys. Chem.* **1964**, *68*, 2772−77.
(15) Shriver, D. F.; Atkins, P. W.; Langford, C. H. *Inorganic Chemistry*, 2nd ed.; Oxford University Press: Oxford/New York, 1994.
(16) Bradshaw, A. M.; Hoffmann, F. M. The Chemisorption of Carbon Monoxide on Palladium Single Crystal Surfaces: IR Spectroscopic Evidence for Localised Site Adsorption. *Surf. Sci.* **1978**, *72*, 513−535.
(17) Kuhn, W. K.; Szanyi, J.; Goodman, D. W. CO Adsorption on Pd(111): The Effects of Temperature and Pressure. *Surf. Sci. Lett.* **1992**, *274*, L611−L618.
(18) Ozensoy, E.; Meier, D. C.; Goodman, D. W. Polarization Modulation Infrared Reflection Absorption Spectroscopy at Elevated Pressures: CO Adsorption on Pd(111) at Atmospheric Pressures. *J. Phys. Chem. B* **2002**, *106*, 9367−9371.
(19) Ohtani, H.; Van Hove, M. A.; Somorjai, G. A. Leed Intensity Analysis of the Surface Structures of Pd(111) and of CO Adsorbed on Pd(111) in a ($\sqrt{3} \times \sqrt{3}$)R30° Arrangement. *Surf. Sci.* **1987**, *187*, 372−386.
(20) Gießel, T.; et al. A Photoelectron Diffraction Study of Ordered Structures in the Chemisorption System Pd111-CO. *Surf. Sci.* **1998**, *406*, 90−102.
(21) Surnev, S.; Sock, M.; Ramsey, M. G.; Netzer, F. P.; Wiklund, M.; Borg, M.; Andersen, J. N. CO Adsorption on Pd(111): A High-Resolution Core Level Photoemission and Electron Energy Loss Spectroscopy Study. *Surf. Sci.* **2000**, *470*, 171−185.
(22) Rose, M. K.; Mitsui, T.; Dunphy, J.; Borg, A.; Ogletree, D. F.; Salmeron, M.; Sautet, P. Ordered Structures of CO on Pd(111) Studied by STM. *Surf. Sci.* **2002**, *512*, 48−60.
(23) Zheng, G.; Altman, E. I. The Oxidation of Pd(111). *Surf. Sci.* **2000**, *462*, 151−168.
(24) Klikovits, J.; Napetschnig, E.; Schmid, M.; Seriani, N.; Dubay, O.; Kresse, G.; Varga, P. Surface Oxides on Pd(111): STM and Density Functional Calculations. *Phys. Rev. B* **2007**, *76*, 045405:1−9.
(25) Kan, H. H.; Weaver, J. F. Mechanism of PdO Thin Film Formation During the Oxidation of Pd(1 1 1). *Surf. Sci.* **2008**, *603*, 2671−2682.
(26) Gabasch, H.; et al. In-situ XPS Study of Pd(111) Oxidation at Elevated Pressure, Part 2: Palladium Oxidation in the 10^{-1} mbar Range. *Surf. Sci.* **2006**, *600*, 2980−2989.
(27) Kan, H. H.; Weaver, J. F. A PdO(1 0 1) Thin Film Grown on Pd(1 1 1) in Ultrahigh Vacuum. *Surf. Sci.* **2008**, *602*, L53−L57.
(28) Martin, N. M.; et al. Dissociative Adsorption of Hydrogen on PdO(101) Studied by HRCLS and DFT. *J. Phys. Chem. C* **2013**, *117* (26), 13510−13519.
(29) Nakai, I.; Kondoh, H.; Shimada, T.; Resta, A.; Andersen, J. N.; Ohta, T. Mechanism of CO Oxidation Reaction on O-covered Pd(111) Surfaces Studied With Fast X-ray Photoelectron Spectroscopy: Change of Reaction Path Accompanying Phase Transition of O Domains. *J. Chem. Phys.* **2006**, *124*, 224712−224717.

(30) Seitsonen, A. P.; Kim, Y. D.; Schwegmann, S.; Over, H. Comprehensive Characterization of the (2 × 2)-O and the CO-Induced ($\sqrt{3} \times \sqrt{3}R30°$-O Overlayers on Pd(111). *Surf. Sci.* **2000**, *468*, 176−186.
(31) Hirvi, J. T.; Kinnunen, T. J.; Suvanto, M.; Pakkanen, T. A.; Nørskov, J. K. CO Oxidation on PdO Surfaces. *J. Chem. Phys.* **2010**, *133*, 084704−084709.
(32) Zorn, K.; Giorgio, S.; Halwax, E.; Henry, C. R.; Grönbeck, H.; Rupprechter, G. CO Oxidation on Technological Pd-Al_2O_3 Catalysts: Oxidation State and Activity. *J. Phys. Chem. C* **2011**, *115*, 1103−1111.
(33) Westerström, R.; et al. Oxidation and Reduction of Pd(100) and Aerosol-Deposited Pd Nanoparticles. *Phys. Rev. B* **2011**, *83*, 115440:1−10.
(34) Hinojosa, J. A., Jr.; Kan, H. H.; Weaver, J. F. Molecular Chemisorption of O_2 on a PdO(101) Thin Film on Pd(111). *J. Phys. Chem. C* **2008**, *112*, 8324−8331.
(35) Over, H. Crystallographic Study of Interaction Between Adspecies on Metal Surfaces. *Prog. Surf. Sci.* **1998**, *58*, 249−376.
(36) Nyholm, R.; Anderssen, J. N.; Johansson, U.; Jensen, B.; Lindau, I. Beamline I311 at MAX-lab: A VUV/Soft X-Ray Undulator Beamline for High Resolution Electron Spectroscopy. *Nucl. Instrum. Methods Phys. Res. A* **2001**, *467−468*, 520−524.
(37) Lundgren, E.; Kresse, G.; Klein, C.; Borg, M.; Andersen, J. N.; De Santis, M.; Gauthier, Y.; Konvicka, C.; Schmid, M.; Varga, P. Two-Dimensional Oxide on Pd(111). *Phys. Rev. Lett.* **2002**, *88*, 246103:1−4.
(38) Devarajan, S. P.; Hinojosa, J. A., Jr.; Weaver, J. F. STM Study of High-Coverage Structures of Atomic Oxygen on Pt(111): p(2 × 1) and Pt Oxide Chain Structures. *Surf. Sci.* **2008**, *602* (19), 3116−3124.
(39) Guo, X. C.; Yates, J. T. Dependence of Effective Desorption Kinetic-Parameters on Surface Coverage and Adsorption Temperature - CO on Pd(111). *J. Chem. Phys.* **1989**, *90* (11), 6761−6766.
(40) Rupprechter, G.; et al. Sum Frequency Generation Vibrational Spectroscopy at Solid−Gas Interfaces: CO Adsorption on Pd Model Catalysts at Ambient Pressure. *Surf. Sci.* **2002**, *502503* (0), 109−122.
(41) Morkel, M.; Rupprechter, G.; Freund, H. J. Ultrahigh Vacuum and High-Pressure Coadsorption of CO and H_2 on Pd(111): A Combined SFG, TDS, and LEED Study. *J. Chem. Phys.* **2003**, *119* (20), 10853−10866.
(42) Bourguignon, B.; Carrez, S.; Dragnea, B.; Dubost, H. Vibrational Spectroscopy of Imperfect CO/Pd(111) Surfaces Obtained by Adsorption Between 150 and 230 K. *Surf. Sci.* **1998**, *418* (1), 171−180.
(43) Perdew, J. P.; Burke, K.; Ernzerhof, M. Generalized Gradient Approximation Made Simple. *Phys. Rev. Lett.* **1996**, *77*, 3865−3868.
(44) Kresse, G.; Hafner, J. Ab Initio Molecular-Dynamics Simulation of the Liquid-Metal-Amorphous-Semiconductor Transition in Germanium. *Phys. Rev. B* **1994**, *49*, 14 251−14271.
(45) Kresse, G.; Furthmüller, J. Efficiency of Ab-Initio Total Energy Calculations for Metals and Semiconductors Using a Plane-Wave Basis Set. *Comput. Mater. Sci.* **1996**, *6*, 15−50.
(46) Kresse, G.; Furthmüller, J. Efficient Iterative Schemes for Ab Initio Total-energy Calculations Using a Plane-Wave Basis Set. *Phys. Rev. B* **1996**, *54*, 11 169−11 186.
(47) Blöchl, P. E. Projector Augmented-Wave Method. *Phys. Rev. B* **1994**, *50*, 17 953−17 979.
(48) Kresse, G.; Joubert, D. From Ultrasoft Pseudopotentials to the Projector Augmented-Wave Method. *Phys. Rev. B* **1999**, *59*, 1758−1775.
(49) Monkhorst, H. J.; Pack, J. D. Special Points for Brillouin-Zone Integrations. *Phys. Rev. B* **1976**, *13*, 5188−5192.
(50) Pack, J. D.; Monkhorst, H. J. "Special Points for Brillouin-Zone Integrations" - A Reply. *Phys. Rev. B* **1977**, *16*, 1748−49.
(51) Pehlke, E.; Scheffler, M. Evidence for Site-Sensitive Screening of Core Holes at the Si and Ge(001) Surface. *Phys. Rev. Lett.* **1993**, *71*, 2338−2341.
(52) Nakamoto, K. *Infrared and Raman Spectra of Inorganic and Coordination Compounds*, 4th ed.; Wiley: New York, 1986.
(53) Ishi, S.-I.; Ohno, Y.; Viswanathan, B. An Overview on the Electronic and Vibrational Properties of Adsorbed CO. *Surf. Sci.* **1985**, *161*, 349−372.
(54) Due to insufficient cancellation of self-interaction between the Hartree and exchange contributions in the functional, the PBE functional is known to overly delocalize electronic states. In the case of CLS, this could result in a too efficient electronic screening of the core hole. Inclusion of Hartree−Fock exchange in the xc-functional could be one way to remedy the problem. We have performed PBE0[55] calculations in order to investigate how such hybrid functionals affect the CLS in the considered systems. These calculations are expensive, and we have only been able to consider selected systems. The shift between a bulk Pd in the metal and the oxide is calculated to be +2.0 eV in PBE0. This was evaluated with a slab consisting of three Pd(100) layers and three PdO(101) layers. The corresponding PBE value is +0.90 eV, and the experimental value is +1.6 eV. Also the C 1s shift is affected by the functional. The shift between CO adsorbed atop at PdO(101) and bridge at Pd(100) is +1.1 (+1.51) eV in PBE (PBE0).
(55) Perdew, J. P.; Enzerhof, M.; Burke, K. Rationale for mixing exact exchange with density functional approximations. *J. Chem. Phys.* **1996**, *105*, 9982−85.
(56) Beutler, A.; Lundgren, E.; Nyholm, R.; Andersen, J. N.; Setlik, B.; Heskett, D. Coverage and Temperature-Dependent Site Occupancy of Carbon Monoxide on Rh(111) Studied by High-Resolution Core-Level Photoemission. *Surf. Sci.* **1998**, *396*, 117−136.
(57) Gao, F.; Lundwall, M.; Goodman, D. W. Infrared Reflection Absorption Spectroscopy Study of CO Adsorption and Reaction on Oxidized Pd(100). *J. Phys. Chem. C* **2008**, *112*, 6057−6064.
(58) Rogal, J.; Reuter, K.; Scheffler, M. CO Oxidation at Pd(100): A First-Principles Constrained Thermodynamics Study. *Phys. Rev. B* **2007**, *75*, 205433:1−11.
(59) Rogal, J.; Reuter, K.; Scheffler, M. Thermodynamic Stability of PdO Surfaces. *Phys. Rev. B* **2004**, *69*, 075421:1−8.
(60) Seriani, N.; Harl, J.; Mittendorfer, F.; Kresse, G. A First-Principles Study of Bulk Oxide Formation on Pd(100). *J. Chem. Phys.* **2009**, *131*, 054701:1−7.
(61) Bradshaw, A. M.; Hoffmann, F. M. The Chemisorption of Carbon Monoxide on Palladium Single Crystal Surfaces: IR Spectroscopic Evidence for Localised Site Adsorption. *Surf. Sci.* **1978**, *72* (3), 513−535.
(62) Kuhn, W. K.; Szanyi, J.; Goodman, D. W. CO Adsorption on Pd(111): The Effects of Temperature and Pressure. *Surf. Sci.* **1992**, *274* (3), L611−L618.
(63) Woodruff, D. P.; Hayden, B. E.; Prince, K.; Bradshaw, A. M. Dipole Coupling and Chemical Shifts in IRAS of CO Adsorbed on Cu(110). *Surf. Sci.* **1982**, *123*, 397−412.
(64) Kasper, N.; Nolte, P.; Stierle, A. Stability of Surface and Bulk Oxides on Pd(111) Revisited by In-situ X-ray Diffraction. *J. Phys. Chem. C* **2012**, *116/40*, 21459−21464.
(65) Over, H.; Kim, Y. D.; Seitsonen, A. P.; Wendt, S.; Lundgren, E.; Schmid, M.; Varga, P.; Morgante, A.; Ertl, G. Atomic-Scale Structure and Catalytic Reactivity of the RuO_2(110) Surface. *Science* **2000**, *287*, 1474−1476.
(66) Kim, Y. D.; Seitsonen, A. P.; Over, H. Adsorption Characteristics of CO and N_2 on RuO_2(110). *Phys. Rev. B* **2001**, *63*, 115419:1−6.
(67) Lundgren, E.; Gustafson, J.; Resta, A.; Weissenrieder, J.; Mikkelsen, A.; Andersen, J. N.; Köhler, L.; Kresse, G.; Klikovits, J.; Biedermann, A.; Schmid, M.; Varga, P. The Surface Oxide as a Source of Oxygen on Rh(111). *J. Electron Spectrosc. Relat. Phenom.* **2005**, *144−147*, 367−372.
(68) Chen, M.; Zheng, Y.; Wan, H. Kinetics and Active Surfaces for CO Oxidation on Pt-Group Metals Under Oxygen Rich Conditions. *Top Catal.* **2013**, *56*, 12991313.